Received: 8 October 2018 | Revised: 14 March 2019 | Accepted: 22 April 2019

DOI: 10.1111/jace.16525

ORIGINAL ARTICLE

Journal of the American Ceramic Society

Demonstration of SiO_2/SiC-based protective coating for dental ceramic prostheses

Zhiting Chen[1] | **Chaker Fares**[1] | **Randy Elhassani**[1] | **Fan Ren**[1] | **Mijin Kim**[2] | **Shu-Min Hsu**[2] | **Arthur E. Clark**[2] | **Josephine F. Esquivel-Upshaw**[2]

[1]Department of Chemical Engineering, University of Florida College of Engineering, Gainesville, Florida

[2]Division of Prosthodontics Gainesville, Department of Restorative Dental Sciences, University of Florida College of Dentistry, Gainesville, Florida

Correspondence
Josephine F. Esquivel-Upshaw, University of Florida College of Dentistry, 1395 Center Drive, Room D9-6, Gainesville, FL 32610.
Email: jesquivel@dental.ufl.edu

Funding information
National Institute of Dental and Craniofacial Research, Grant/Award Number: R01 DE025001

Abstract

SiO_2/SiC coatings were deposited onto ceramics disks using plasma-enhanced chemical vapor deposition. The effects of deposition pressure and gas-flow ratio on the refractive index, extinction coefficient, and SiC composition were studied. For the highest studied SiH_4 to CH_4 gas-flow ratio of 1.5, the refractive index increased by 17% from 2.53 (at the wavelength of 845 nm) to 2.96 (at the wavelength of 400 nm). For the lowest studied SiH_4 to CH_4 gas-flow ratio of 0.5, the refractive index only increased by 4% from 2.11 (at the wavelength of 845 nm) to 2.20 (at the wavelength of 400 nm). At higher deposition pressures, the variation in refractive index of the SiC coatings was significantly lower showing a slight increase from 1.93 (at a wavelength of 845 nm) to 1.96 at a wavelength of 400 nm. Except for the case of a low SiH_4 to CH_4 gas-flow ratio of 0.5, for light with wavelengths $\leq$650 nm, the extinction coefficient of the SiC coatings increased significantly. Light with a wavelength >650 nm had an extinction coefficient near 0 in all cases. After annealing the sample at 400°C for 4 hours, hydrogen-related bonds broke and the stress of the film was reduced from −245 to −71 MPa. By utilizing different thicknesses of SiC, the full standard dental shade guide was matched with the ΔE of each coated disk being less than 3.3 compared to the shade guide.

KEYWORDS
applications, chemical vapor deposition, coatings

1 | INTRODUCTION

Glass-based ceramic materials have been widely used for fixed dental prostheses (FDPs) such as crowns or bridges.[1–3] In practice, these ceramics need to have good biocompatibility, realistic aesthetics, and superior durability to ensure longevity within the patient's mouth. In previous reports, mechanical and chemical abrasiveness have been shown to cause roughened surfaces on glass-based ceramics.[4–6] These roughened surfaces result in an accelerated rate of biofilm/plaque accumulation and excessive wear of the opposing enamel/FDP.[4–6] The increased wear on the ceramic surface also causes rapid loss of surface structure and decreases flexural strength through glass-phase degradation, making the FDPs susceptible to chipping failures.[6,7] All of these issues can decrease the longevity of the ceramic-based restoration and damage adjacent oral structures. To mitigate surface roughening and chipping problems, monolithic zirconia has been employed as an alternative to glass-based ceramics because of this material's high hardness and flexural strength.[8,9] Despite many advantages of monolithic zirconia, high temperature sintering of the ceramic causes oxygen vacancies to be generated, which results in discoloration of the material.[10,11] Proper color matching to the desired dental shade is

difficult because of the discoloration of monolithic zirconia FDPs. In order to improve the reliability and success rate of many dental applications, the use of a material that is durable, biocompatible, and can be manufactured to easily match dental tooth shades is desirable.

Instead of introducing new ceramics, another approach is to apply deposited coatings to existing ceramic materials. An ideal coating would be minimally abrasive toward enamel, therefore increasing the longevity of the coated ceramic-based FDPs. Additionally, the coated material's thickness can be modified to provide different shades to match any application within the dental field. Out of the many material coatings that could be used, amorphous SiC seems to be the most promising because of this material's excellent mechanical and corrosion resistant properties as compared to standard silicon-based oxide or nitride coatings.[12–15]

Beyond SiC's material properties, this material has been studied and applied as a viable biomaterial in the literature.[16,17] One study showed that SiC appears to be cytocompatible on both basal and specific cyctocompatability levels.[18] Another study showed that amorphous SiC showed no cycotoxicity when incubated for 24 hours with mice fibroblasts L929 cell cultures.[19] With regard to the dental field, no previous research has been done on SiC-based coatings, but some reports have been published on the incorporation of SiC into other dental materials. Higashiguchi et al[20] evaluated the possibility of dental implant application of SiC by embedding SiC in the drilled hole of the rat femurs. Between 1 and 3 weeks, Higashiguchi reported callusing followed by fibrous tissue regenerating between the SiC and encapsulating bone surface with a similar morphology to traditional bone-ceramic interfaces.[20]

There are several methods for SiC film depositions including sputtering,[21] plasma spray,[22] chemical vapor deposition (CVD),[23] and plasma-enhanced chemical vapor deposition (PECVD)[12] Using CVD or PECVD deposition, the mechanical and optical properties of the deposited SiC film can be easily adjusted by altering the ratio of the gas precursors used. Typically, the SiC films deposited with PECVD are amorphous hydrogenated SiC.[23]

In this work, the effects of SiC deposition conditions on the optical properties and composition of SiC were investigated. The ability to match the colors of glass-ceramic-based (Zirpress, Ivoclar Vivadent, Schaan) materials with different thicknesses of deposited SiO_2/SiC layers were studied. The SiO_2/SiC film stress and adhesion on these disks were also evaluated.

2 | MATERIALS AND METHODS

2.1 | Dielectric film deposition

SiO_2 and SiC film depositions were performed with a Plasma-Enhanced Chemical Vapor Deposition (PECVD, PlasmaTherm 790, Saint Petersburg, FL) system at 300°C. Precursors for SiO_2 and SiC film depositions were silane/nitrous oxide and silane/methane, respectively. The PECVD system has a parallel plate configuration with a shower head with a load lock, and the maximum deposition temperature is 350°C.. The deposition pressure was varied from 850 to 1100 mTorr. The deposition rate was 340 Å/min for SiO_2 and 165 Å/min for SiC. The self-bias voltage was between 0 and 3 V for both films. The diameter of the sample tray is 305 mm and the system can accommodate 4 of 4" wafer.

2.2 | Dielectric film characterizations

The SiO_2 and SiC film thickness, refractive index (n), and extinction coefficient (k) were determined with a photospectrometer (Filmetrics F40, San Diego CA). The model used to determine n and k utilized an amorphous dispersion model. The film stress, σ_f, was determined using a profilometer (Dektak 150, Veeco, St. Paul MN) to measure the curvature of a 2" silicon wafer with and without a SiO_2 or SiC film. Then, σ_f can be calculated using the Stoney equation by taking into account the radius of curvature before and after film deposition.[24,25] The Stoney equation is shown below,

$$\sigma_f = \frac{E_s \times d_s^2}{6\left(1-\nu_s\right)} \times \frac{1}{d_f} \times \left(\frac{1}{R_{post}} - \frac{1}{R_{pre}}\right) \quad (1)$$

where E_s and ν_s are Young's modulus and Poisson's ratio of the silicon wafer, respectively. d_s is the thickness of the silicon wafer, and *df* is the thickness of dielectric film. R_{pre} and R_{post} are the radii of curvature before and after film deposition, respectively. The composition of the SiC was determined with energy-dispersive x-ray spectroscopy (EDS) in a scanning electron microscope (SEM). For the EDS measurements, SiC was deposited on GaAs substrates so that the corresponding Si and C concentrations were exclusively from the SiC layer along with a standard and matrix corrections to improve accuracy to ~2%. Analysis of several samples at each condition was utilized to ensure precise results. Matrix corrections along with a standard were utilized to improve the accuracy of the measurement.[26]

Fourier Transform Infrared Spectroscopy (Thermo Electron Magna 760) was used to determine the chemical composition of the SiC after deposition.

To investigate the capability of the SiO_2/SiC coatings for different color shades, 12 mm × 2 mm glass-ceramic disks (IPS Zirpess, Ivoclar Vivadent, Schaan, Liechtenstein) were used as substrates to coat different thickness of SiO_2 and SiC layers. Prior to the coating process, the disks were cleaned with acetone in an ultrasonic bath, rinsed with isopropyl

alcohol, and dried using compressed nitrogen. A spectrophotometer (Chroma meter CR-300, Minolta, Osaka, Japan) was used to determine the color difference (ΔE_{ab}) between a standard shade guide (Vita standard shade guide, Vita Zahnfabrik, Bad Sackingen, Germany) and the SiO_2/SiC coated ceramic disks. To consider a coated disk to visually match the Vita shade guide, a ΔE_{ab} value less than 3.3 was required.[27] The color difference calculation is derived from the formula shown in Equation 2:[27]

$$\Delta E_{ab} = \sqrt{(\Delta L^*)^2 + (\Delta a^*)^2 + (\Delta b^*)^2} \quad (2)$$

where L* is the lightness, a* is the green/red color component, b* is the yellow/blue color component. ΔL*, Δa*, and Δb* indicate differences in L*, a*, and b* between a standard and a test sample.

2.3 | Wear resistance of SiC coatings

The wear resistance of the coated disks were tested using a chewing simulator (CS Mechatronik GMBH). The coated and non-coated glass-ceramic disks were opposed with a steatite ball under 49 N load for 3200, 6400, and 15 000 cycles with a lateral speed of 30 mm/s and a horizontal movement of 2.0 mm. The deepest vertical loss (μm) and volume loss (mm^3) were measured using a surface profilometer (KLA-Tencor, Alpha-Step 500) and calculated.

3 | RESULTS

In order to adjust the color of the coated ceramic, two materials with different refractive indices must be utilized. The difference in refractive indices between the two materials allows for easier color variation in the composite coating. In this study, a 20-nm layer of PECVD SiO_2 with a refractive index of 1.45 was deposited onto the glass-ceramic prior to SiC deposition. The glass-ceramic substrates undergo the deposition of both materials in the same chamber and are under vacuum for the duration of the process to avoid contamination. The thin layer of SiO_2 not only makes color matching the substrate easier, this also improves adhesion between the SiC and dental ceramic.

Figure 1A shows the refractive index as a function of wavelength and Figure 1B shows the extinction coefficient as a function of wavelength. Both figures demonstrate the SiH_4:CH_4 gas flow ratios during SiC deposition. For higher SiH_4 to CH_4 ratios, the refractive index showed a larger variation at different wavelengths of light. For a SiH_4 to CH_4 gas flow ratio of 1.5, the refractive index changed by 17% from 2.46 (at a wavelength of 845) to 2.95 (at a wavelength of 400 nm). For the lowest SiH_4 to CH_4 gas flow ratio of 0.5, the refractive index only increased by 4% from 2.11 (at a wavelength of 845) to 2.20 (at a wavelength of 400 nm). When light goes from air to a denser medium such as SiC, the velocity of light decreases and the light bends depending on the refractive index of the denser material. Therefore, a smaller variation of refractive index across the visible wavelength means light is bent less when traveling through the material. Thus, the deposition conditions yielding a smaller variation of refractive index is desirable for these coatings due to a consistent perceived color across the full visible spectrum. In addition to the refractive index, the extinction coefficient of a material has a significant impact on the visual appearance of the coatings. Coatings with higher extinction coefficients will absorb a majority of incident light resulting in a darker color of the coated

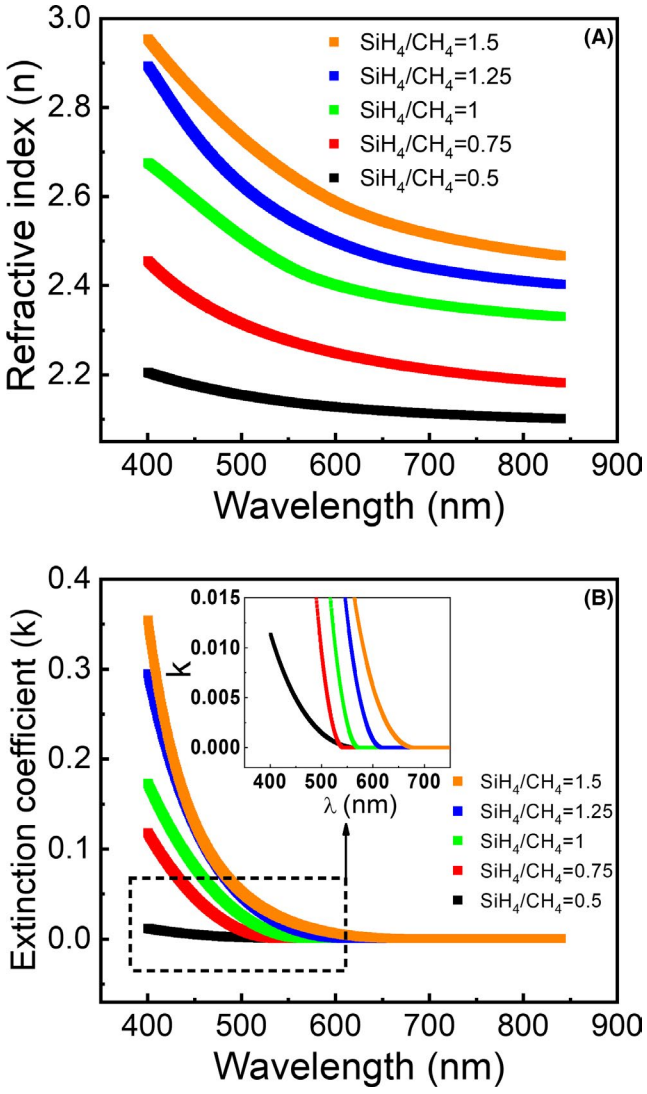

FIGURE 1 (A) Refractive index and (B) extinction coefficient as a function of wavelength for SiC films deposited at 300°C with different gas flow ratios of SiH_4 to CH_4. The insert figure shows the extinction coefficient in the lower wavelength range

ceramics. As shown in Figure 1b, the extinction coefficient is approximately zero for wavelengths larger than 650 nm at all tested SiC deposition conditions. An extinction coefficient near zero means that all incident light will either be transmitted or reflected with minimal absorption. For light with wavelengths ≤650 nm, the extinction coefficient of the SiC coatings increased significantly with the exception of the SiC coatings deposited at the lowest SiH_4:CH_4 gas-flow ratio of 0.5. The inset of Figure 1B illustrates the extinction coefficient of SiC at a gas-flow ratio of 0.5. At a wavelength of 400 nm, the extinction coefficient is 0.01 which means only 1% of the 400 nm light would be absorbed by the SiC coating. Table 1 shows the composition of SiC deposited with different SiH_4 to CH_4 gas flow ratios. As the SiH_4 to CH_4 gas-flow ratio was reduced, the composition of Carbon within the SiC increased.

Figure 2A,B illustrate the effect of deposition chamber pressure on the refractive index and extinction coefficient of the coated materials. At higher deposition pressures, the variation in refractive index of the SiC coatings was significantly lower. For example, Figure 2A shows that the refractive index only slightly increased from 1.93 (at a wavelength of 845) to 1.96 (at a wavelength of 400 nm). Figure 2B shows the extinction coefficient of the SiC coatings deposited at different pressures. High deposition pressure also decreased the extinction coefficient of the deposited layers. As depicted in the inset of Figure 2B, the extinction coefficient of the SiC coating was further reduced to less than 0.05% at a deposition pressure of 1100 mTorr. Figure 3 shows the surface morphology of a glass-ceramic disk before and after a 200 nm coating of SiC. The surface morphology stays relatively constant due to the conformal nature of PECVD depositions.[28,29]

Figure 4 shows an FTIR spectrum of PECVD deposited SiC using a deposition pressure of 1100 mTorr and a Silane:Methane ratio of 0.5. The intense peak that appears at 790 cm^{-1} is attributed to Si-C stretching vibrations. The smaller peaks that appear near 2000-2200 cm^{-1} and 2890 cm^{-1} correspond to Si-H_n stretching mode vibrations (n = 1,2), and stretching mode vibrations of C-H_2 and C-H_3, respectively.[30–32] The spectra of the amorphous SiC utilized within this study agreed with the literature. The hydrogen incorporation in PECVD deposited SiC contributes to a lower hardness compared to SiC grown using other methods.[33]

Figure 5 showed the wear results of the SiO_2/SiC coating at different chewing cycles. The wear resistance of coated disks was around 25 to 30% higher than that of the uncoated ceramic disk at 15,000 cycles for vertical loss (μm) and volume loss (mm^3). Figure 6A illustrates a microscopic picture of a 1.5 mm by 3.3 mm indentation on a SiO_2/SiC coated disk after grinding 15,000 cycles on a chewing simulator. Figure 6B-D show the cross sectional and 45° view SEM pictures aournd the cleaved edge as well as the SEM picture away from the cleaved edge of SiO_2/SiC coated disk, respectively.

TABLE 1 C to Si ratio as a function of SiH_4/CH_4 gas flow ratio at a constant pressure of 850 mTorr and C to Si ratio as a function of deposition pressure at a constant SiH_4/CH_4 gas flow ratio of 0.5

SiH_4/CH_4 Gas Flow Ratio	0.50	0.75	1.00	1.25	1.50
C/Si Atomic Ratio	1.16	0.94	0.79	0.55	0.56
Deposition Pressure (mTorr)	600	725	850	975	1100
C/Si Atomic Ratio	0.88	0.94	1.16	1.16	1.35

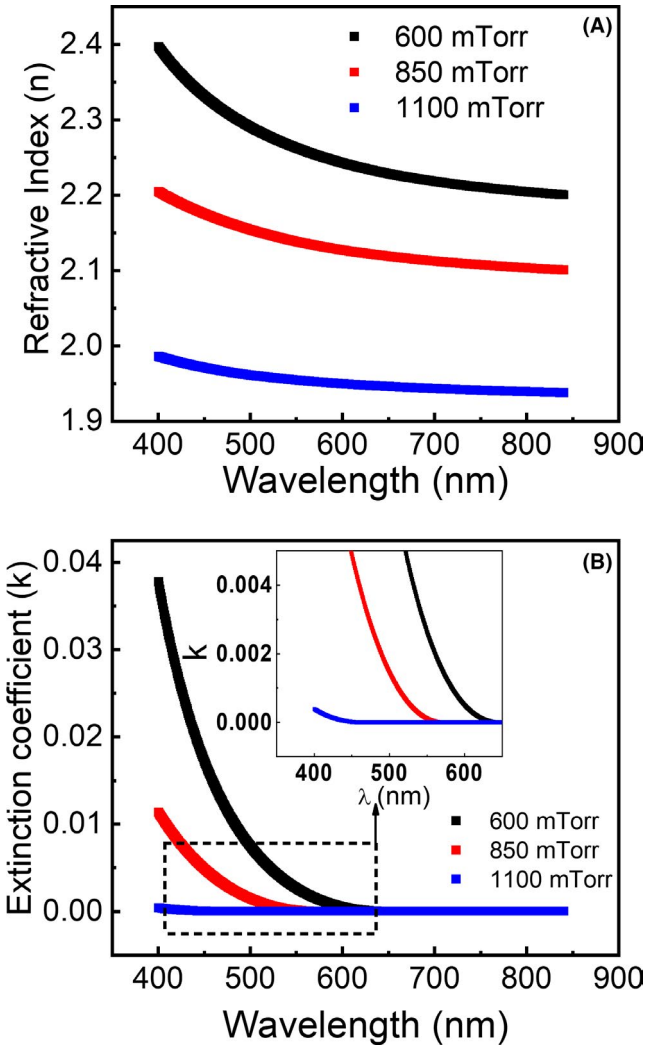

FIGURE 2 (A) Refractive index and (B) extinction coefficient as a function of wavelength for SiC films deposited at 300°C at different deposition pressures. The insert figure shows the extinction coefficient in the lower wavelength range

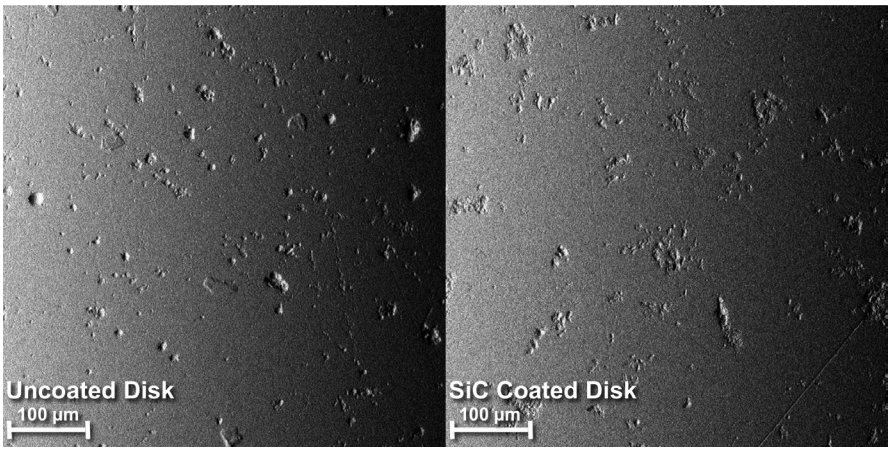

FIGURE 3 SEM pictures of surface morphology before and after PECVD SiO_2/SiC coatings

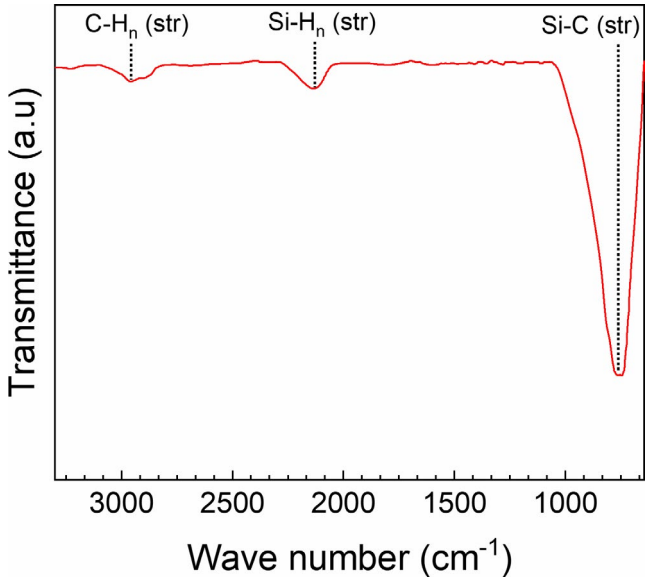

FIGURE 4 FTIR transmittance spectra of a-SiC grown using plasma-enhanced chemical vapor deposition

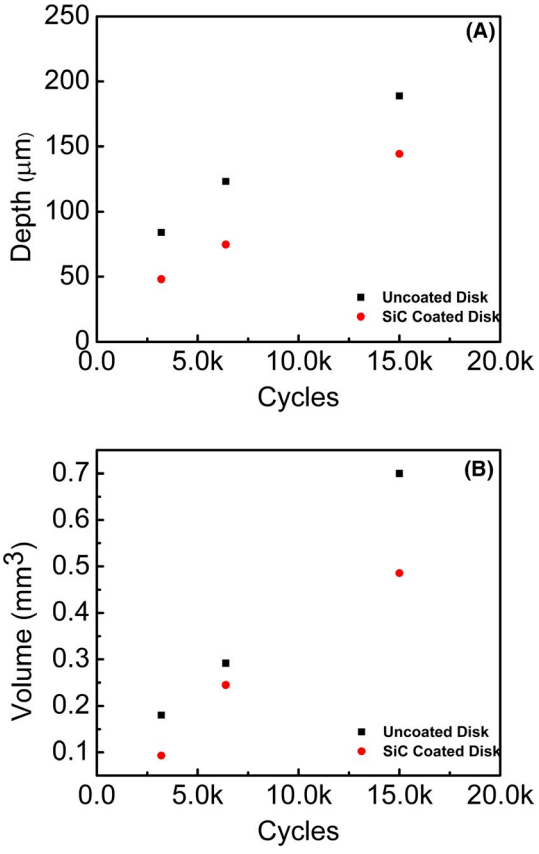

FIGURE 5 Wear results of uncoated disks and SiO_2/SiC-coated disks at different cycles on a chewing simulator, (A) depth (µm) and (B) volume loss (mm^3)

Figure 7 shows glass-ceramic disks with varying thicknesses of deposited SiC used to match colors for the entire Vita standard shade guide. The first row of the table in Figure 7 describes the initial shade of the disk used prior to any coating. The second row illustrates the thickness of the SiC film after depositing a fixed thickness of 20 nm SiO_2. The third row of the table shows the color differences, ΔE_{ab}, between the coated disks and VITA shade guide. All the ΔE_{ab} are less than 3.3, which indicates the coated disks are visually acceptable when compared to the Vita shade guide.

Figure 8 shows the contour of a bare 2" silicon wafer, 2" silicon wafer coated with 240 nm of SiC film, and a 2" silicon wafer coated with 240 nm of SiC film then annealed at 400°C for 20 min. After the SiC coating, the contour of the Si wafer became more concave, and the height of curvature across the wafer only increased from 16 to 26 µm. After annealing, the 26 nm height of curvature was reduced to 18 nm. The change in contour of the Si wafer indicated that the PECVD deposited SiC coating was compressive and caused the wafer curvature to become concave. The curvatures of these wafers were simulated with 5th order polynomial equations and the radii of were determined for the SiC film stress using the Stoney Equation.[34] The SiC film

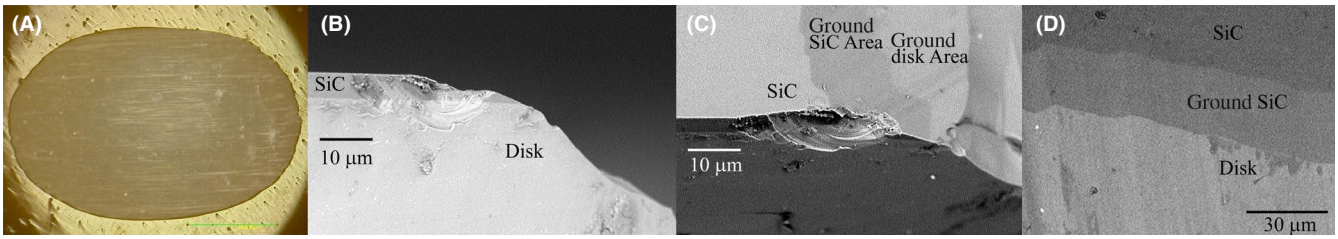

FIGURE 6 (A) A microscopic picture of a wear indentation on SiO_2/SiC coated disk after grinding 15,000 cycles on a chewing simulator; (B) A cross-sectional view SEM picture of a cleaved disk coated with SiO_2/SiC; (C) 45° view of a SEM picture of a cleaved edge on a ceramic disk coated with SiO_2/SiC; (D) 45° view of a SEM picture away from the cleaved edge on a ceramic disk coated with SiO_2/SiC

	A1	A2	A3	A3.5	A4	B1	B2	B3	B4	C1	C2	C3	C4	D2	D3	D4
Substrate	BL2	B1	A1	A1	B3	BL2	A1	A1	A1	B1	B2	A3.5	A3.5	B2	B1	B1
SiC (nm)	125	150	175	325	150	133	135	155	300	100	180	75	280	71	200	230
ΔE	2.98	2.02	2.39	1.46	2.90	1.50	1.66	2.39	2.01	0.88	2.29	2.82	1.97	1.29	1.99	1.08

FIGURE 7 Substrate, SiC thickness, and corresponding ΔE of each coated disk that was matched to the Vita shade Guide. A constant thickness of 20nm SiO_2 was utilized prior to SiC deposition

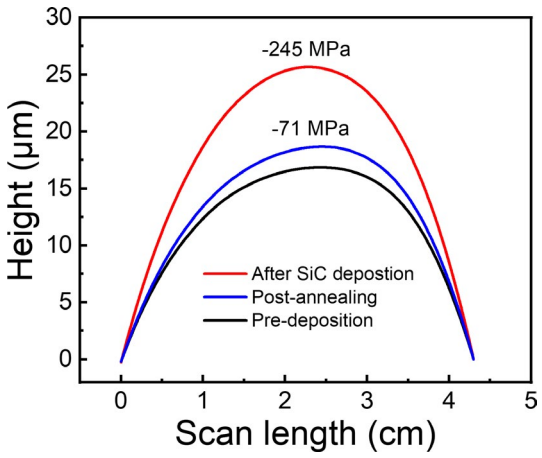

FIGURE 8 Curvature of a 2" silicon wafer coated with 200 nm SiC before and after annealing at 400°C for 20 min

exhibited a stress of 245 MPa which was reduced to 71 MPa after annealing.

4 | DISCUSSION

The most important optical properties for the coated materials are refractive index and extinction coefficient. Refractive index is defined as speed of light in a vacuum divided by the speed of light in the medium and is used to determine the degree of light wave bending when light travels through different materials.[35] Extinction coefficient is the measurement of light absorption depending on the mass density or molar concentration of a specific substance. In order to match color of the SiC protective coating to each color in the Vita shade guide, a second coating layer with a different refractive index is needed. Altering the final color in the composite coating is easier when there is a greater difference in the refractive index between two materials. Prior to the deposition of SiC, a 20-nm layer of SiO_2 was used as the second coated layer with a different refractive index deposited using SiH_4 and N_2O precursors. The refractive index of SiO_2 is 1.45, and the extinction coefficient is approximately zero across the entire visible light spectrum. SiO_2 makes up approximately 50%-60% of the dental ceramics used in this study, therefore the thin SiO_2 layer also enhances adhesion between the SiC and dental ceramic through O-Si-O bonds. After the deposition of SiO_2, SiC was deposited directly after without breaking vacuum. The refractive indices of SiC layers deposited in this study are above 2. Deposited materials with refractive indices that are relatively constant across the visible light spectrum and a minimal extinction coefficient is desirable for dental ceramic coatings. Coatings with a refractive index dependent on wavelength will visually appear to be different colors depending on the viewing angle. As shown in Figure 1A, SiC deposited with a SiH_4:CH_4 gas-flow ratio of 0.5 exhibited the smallest variation in refractive index with a 4% increase from 2.11 to 2.20 at wavelengths between 400 and 845 nm. Due to this minimal increase, a 0.5 gas-flow ratio of SiH_4:CH_4 was used for the color matching portion of this study. The other important prerequisite of optimal ceramic coatings is utilizing coatings with low extinction

coefficients. Coated materials with a large extinction coefficient will absorb a majority of incident light, causing the film to be dark in color. If the magnitude of the extinction coefficient is dependent on wavelength, the color of the dielectric films will also be different when viewed at different angles. As shown in Figure 1B, the extinction coefficient of all the SiC deposition conditions are wavelength dependent in the wavelength range from 400 to 550 nm and are nearly zero for wavelengths larger than 650 nm. As shown in the inset of Figure 1B, SiC deposited with a SiH_4 to CH_4 gas-flow ratio of 0.5 displayed the lowest extinction coefficient of 0.1 at 400 nm. In addition to the SiH_4:CH_4 gas-flow ratio, the SiC deposition pressure also affects both the refractive index and extinction coefficient, as shown in Figure 2. When the deposition pressure increases, the refractive indices were less dependent on wavelength and the extinction coefficient became smaller.

The PECVD deposited SiC is amorphous and hydrogenated.[34] The atomic composition of the SiC film is highly reliant on the deposition conditions. As illustrated in Table 1, higher deposition pressures and lower SiH_4:CH_4 gas-flow ratios yield a higher concentration of carbon atoms within the SiC film. The energy bandgap of single crystal SiC is approximately 3.2 eV, which is equivalent to a light wavelength of 387 nm. Therefore, light with wavelengths larger than 387 nm do not have sufficient energy to be absorbed by the SiC and the refractive index will not be affected by visible light (390-700 nm). However, for amorphous PECVD deposited SiC, the energy bandgap may be smaller than 3.2 eV ranging from 2.35 to 2.85 as a function of the ratio of SiH_4 to CH_4 flow rate determined with Tauc plots, as the Si content is increased in the SiC film, the energy bandgap of the SiC films becomes smaller.[26,36,37] Since the ratio of SiH_4 to CH_4 flow rate used in our study was 0.5, a energy bandgap of 2.13 eV was determined with Tauc plots. This notion agrees with our experimental results that as the flow ratio is reduced, the Si composition increases, which corresponds to a lower refractive index and lowerer bandgap. Previous research groups also proved that carbon concentration within SiC increased as deposition pressure increases, therefore increasing the SiC bandgap. As shown in Figure 2, this trend is consistent with results shown in this study.

As shown in Figure 3, there were no changes in the surface morphology of a glass-ceramic disk before and after SiO_2/SiC coatings to the conformal nature of PECVD depositions. In addition, there was no peeling observed after the SiO_2/SiC coating grinded on a chewing simulator for 15,000 cycles. As previously mentioned, two coated films with different refractive indices need to be employed to be able to color match the Vita shade guide. Before depositions took place, TFcal Reflectance simulations were used to determine the predicted color of the composite materials as a function of each layer's thickness. The goal of these simulations was to find the specific thickness of SiC to have a reflectance of light to be the white light, which corresponds to a chromaticity coordinate of (1/3, 1/3) on the color chart.

As shown in Figure 7, by varying the SiC thickness along with a fixed 20 nm layer of SiO_2, all 16 color shades were matched with a ΔE less than 3.3 using shades Al, A3.5, B1, B2, and BL2 of glass-ceramic substrates. BL2 disks were used as the substrates for matching the lightest shade guide colors, A1 and B1. A majority of the shade guide could be matched by using A1 or B1 disks as the substrate. A few of shades with a dark color needed darker substrates such as A3.5, B2, or B3 to be matched.

Besides being able to color match the coated disks to the Vita shade guide, good adhesion of the deposited SiC to the ceramic-glass is also an important prerequisite of dental ceramic coatings. The major component of the ceramic-glass is SiO_2 (>50%-60%) and therefore the PECVD deposited SiO_2 serves as a good adhesion layer between the SiC and ceramic substrate via O-Si-O bonds. In addition to chemical bonding, the stress of the PECVD SiO_2 and SiC films also could affect the adhesion of the coated materials to the dental ceramic. Typically, a coated film with tensile stress could suffer peeling issues whereas, a compressive film would could aid in the film adhering the ceramic surface. Thus, deposition conditions were altered to achieve compressive films in this study. To determine how deposition conditions affected the final stress in the deposited films, SiC was coated onto 2" Silicon wafers and the curvature was measured post-deposition. As shown in Figure 8, the curvature of the SiC coated Si wafer became more concave than the uncoated Si wafer and exhibited a compressive stress of 245 MPa. After annealing the sample at 400°C for 4 hours, hydrogen-related bonds broke and the stress of the film was reduced from −245 to −71 MPa.

5 | CONCLUSION

Plasma-enhanced chemical vapor deposited SiO_2/SiC coatings were utilized to coat dental ceramics. The effects of SiH_4 to CH_4 gas-flow ratio and deposition pressure on the SiC composition, refractive index, and extinction coefficient were investigated. The refractive index of SiC films deposited at 1100 mTorr with the SiH_4 to CH_4 flow ratio of 0.5 exhibited minimal variations of refractive index from 2.11 to 2.20 for the entire visible light spectrum. Using these conditions, the extinction coefficient of the deposited SiC was close to zero which means a negligible amount of incident light would be absorbed. By employing a 20 nm SiO_2 layer along with different thickness of SiC, the entire Vita shade guide was able to be matched with each ΔE being less than 3.3. The stress of the SiC film was measured and determined to be a compressive stress of −245 MPa. By annealing the

SiC at 400°C for 20 minutes, the stress of SiC film was reduced to −71 MPa.

ACKNOWLEDGMENTS

NIH-NIDCR Grant R01 DE025001 supported this study. Ceramic materials were supplied by Ivoclar Vivadent. SEM-EDAX was performed at the Major Analytical Instrumentation Center of the University of Florida.

CONFLICT OF INTEREST

There are no conflicts of interest associated with this research project.

ORCID

Josephine F. Esquivel-Upshaw https://orcid.org/0000-0003-3642-8087

REFERENCES

1. Tian T, Tsoi JKH, Matinlinna JP, Burrow MF. Aspects of bonding between resin luting cements and glass ceramic materials. Dent Mater. 2014;30(7):e147–e162.
2. Sailer I, Makarov NA, Thoma DS, Zwahlen M, Pjetursson BE. All-ceramic or metal- ceramic tooth-supported fixed dental prostheses (FDPs)? A systematic review of the survival and complication rates. Part I: Single crowns (SCs). Dent Mater. 2015;31(6):603–23.
3. Silva LHd, Lima Ed, Miranda RBdP, Favero SS, Lohbauer U, Cesar PF. Dental ceramics: a review of new materials and processing methods. Braz Oral Res. 2017;31:133–46.
4. Anusavice KJ, Kakar K, Ferree N. Which mechanical and physical testing methods are relevant for predicting the clinical performance of ceramic-based dental prostheses? Clin Oral Implants Res. 2007;18(s3):218–31.
5. Sailer I, Gottnerb J, Kanelb S, Hammerle CH. Randomized controlled clinical trial of zirconia-ceramic and metal-ceramic posterior fixed dental prostheses: a 3-year follow-up. Int J Prosthodont. 2009;22(6):553–60.
6. Esquivel-Upshaw JF, Dieng FY, Clark AE, Neal D, Anusavice KJ. Surface degradation of dental ceramics as a function of environmental pH. J Dent Res. 2013;92(5):467–71.
7. Esquivel-Upshaw JF, Ren F, Hsu SM, Dieng FY, Neal D, Clark AE. Novel testing for corrosion of glass-ceramics for dental applications. J of Dent Res. 2018;97(3):296–302.
8. Sripetchdanond J, Leevailoj C. Wear of human enamel opposing monolithic zirconia, glass ceramic, and composite resin: an in vitro study. J Prosthet Dent. 2014;112(5):1141–50.
9. Nakamura K, Harada A, Inagaki R, Kanno T, Yoshimi N, Milleding P, et al. Fracture resistance of monolithic zirconia molar crowns with reduced thickness. Acta Odontol Scand. 2015;73(8):602–8.
10. Langer J, Hoffmann MJ, Guillon O. Electric field-assisted sintering in comparison with the hot pressing of yttria-stabilized zirconia. J Am Ceram Soc. 2011;94(1):24–31.
11. Ebeid K, Wille S, Hamdy A, Salah T, El-Etreby A, Kern M. Effect of changes in sintering parameters on monolithic translucent zirconia. Dent Mater. 2014;30(12):e419–e424.
12. Müller G, Krötz G, Niemann E. SiC for sensors and high-temperature electronics. Sensors Actuators A Phys. 1994;43(1):259–68.
13. Flannery AF, Mourlas NJ, Storment CW, Tsai S, Tan SH, Heck J, et al. PECVD silicon carbide as a chemically resistant material for micromachined transducers. Sensors Actuators A Phys. 1998;70(1):48–55.
14. Sarro PM. Silicon carbide as a new MEMS technology. Sensors Actuators A Phys. 2000;82(1):210–8.
15. Ivashchenko VI, Turchi PEA, Shevchenko VI. Simulations of the mechanical properties of crystalline, nanocrystalline, and amorphous SiC and Si. Phys Rev B. 2007;75(8):085209.
16. Saddow SE. Silicon carbide materials for biomedical applications. In: Silicon Carbide Biotechnology, 2nd edn. Saddow SE (ed). Waltham, MA: Elsevier; 2016: pp. 1–25.
17. Kotzar G, Freas M, Abel P, Fleischman A, Roy S, Zorman C, et al. Evaluation of MEMS materials of construction for implantable medical devices. Biomaterials. 2002;23(13):2737–50.
18. Naji A, Harmand MF. Cytocompatibility of two coating materials, amorphous alumina and silicon carbide, using human differentiated cell cultures. Biomaterials. 1991;12(7):690–4.
19. Amon M, Bolz A, Schaldach M. Improvement of stenting therapy with a silicon carbide coated tantalum stent. J Mater Sci Mater Med. 1996;7(5):273–8.
20. Hashiguchi K, Hashimoto K. Mechanical and histological investigations on pressureless sintered SiC dental implants. Okajimas Folia Anat Jpn. 1999;75(6):281–96.
21. Rovira PI, Alvarez F. Chemical (dis)order in a-Si1-xCx: H for x<0.6. Phys Rev B. 1997;55(7):4426–34.
22. Kang HK, Kang SB. Thermal decomposition of silicon carbide in a plasma-sprayed Cu/SiC composite deposit. Mater Sci Eng A. 2006;428(1):336–45.
23. Powell JA, Larkin DJ. Process-induced morphological defects in epitaxial CVD silicon carbide. Phys Status Solidi B. 1997;202(1):529–48.
24. Stoney GG. The tension of metallic films deposited by electrolysis. Proceedings of the Royal Society of London Series A, Containing Papers of a Mathematical and Physical Character. London: Royal Society; 1909:p. 172–5.
25. Wuu DS, Horng RH, Chan CC, Lee YS. Plasma-deposited amorphous silicon carbide films for micromachined fluidic channels. Appl Surf Sci. 1999;144–145:708–12.
26. Goldstein JI, Newbury DE, Michael JR, Ritchie NWM, Scott JHJ, Joy DC. Scanning electron microscopy and X-ray microanalysis. New York, NY: Springer; 2017.
27. McLaren K. XIII-The development of the CIE 1976 (L* a* b*) uniform colour space and colour-difference formula. J Soc Dye Colour. 1976;92(9):338–41.
28. Maeda K, Fisher SM. CVD TEOS/O3: development history and applications. Solid State Technol. 1993;36(6):83–8.
29. Silva ANRd, Morimoto NI. Gas flow simulation in a PECVD reactor. In Proceedings of the 2002 International Conference on Computational Nanoscience and Nanotechnology. San Juan, Puerto Rico: TechConnect Briefs; 2002:p. 22–5.
30. Kim MT, Lee J. Characterization of amorphous SiC: H films deposited from hexamethyldisilazane. Thin Solid Films. 1997;303(1–2):173–9.

31. Kaneko T, Nemoto D, Horiguchi A, Miyakawa N. FTIR analysis of a-SiC: H films grown by plasma enhanced CVD. J Cryst Growth. 2005;275(1):e1097–e1101.
32. Kim DS, Lee YH. Room-temperature deposition of a-SiC: H thin films by ion-assisted plasma-enhanced CVD. Thin Solid Films. 1996;283(1–2):109–18.
33. Frischmuth T, Schneider M, Maurer D, Grille T, Schmid U. High temperature annealing effects on the chemical and mechanical properties of inductively-coupled plasma-enhanced chemical vapor deposited a-SiC: H. Thin Solid Films. 2016;611:6–11.
34. Feng X, Huang Y, Rosakis AJ. On the stoney formula for a thin film/substrate system with nonuniform substrate thickness. J Appl Mech. 2007;74(6):1276–81.
35. Heffernan MJ, Aquilino SA, Diaz-Arnold AM, Haselton DR, Stanford CM, Vargas MA. Relative translucency of six all-ceramic systems. Part II: Core and veneer materials. J Prosthet Dent. 2002;88(1):10–5.
36. Daves W, Krauss A, Behnel N, Häublein V, Bauer A, Frey L. Amorphous silicon carbide thin films (a-SiC: H) deposited by plasma-enhanced chemical vapor deposition as protective coatings for harsh environment. Thin Solid Films. 2011;519(18):5892–8.
37. Pham HTM, Akkaya T, Boer Cd, Visser CCG, Sarro PM. Electrical and optical properties of PECVD SiC thin films for surface micromachined devices. In SAFE 2002 Proceedings of 5th Semiconductor Advances for Future Electronics Workshop. Utrecht, The Netherlands: STW Technology Foundation, 2002: p. 662–6.

How to cite this article: Chen Z, Fares C, Elhassani R, et al. Demonstration of SiO_2/SiC-based protective coating for dental ceramic prostheses. *J Am Ceram Soc*. 2019;00:1–9. https://doi.org/10.1111/jace.16525